Supporting Information

Electrochemical Modeling of GITT Measurements for Improved Solid-State Diffusion Coefficient Evaluation

Jeffrey S. Horner,[†] Grace Whang,[‡] David S. Ashby,[¶] Igor V. Kolesnichenko,[§] Timothy N. Lambert,[§] Bruce S. Dunn,[‡] A. Alec Talin,[¶] and Scott A. Roberts[*,†]

[†]*Thermal/Fluid Component Sciences Department, Sandia National Laboratories, Albuquerque, New Mexico, USA*

[‡]*Materials Science and Engineering Department, University of California, Los Angeles, Los Angeles, California, USA*

[¶]*Quantum and Electronic Materials Department, Sandia National Laboratories, Livermore, California, USA*

[§]*Photovoltaics and Materials Technology Department, Sandia National Laboratories, Albuquerque, New Mexico, USA*

E-mail: sarober@sandia.gov

Derivation for Exponential Method

The exponential fit method used in this paper can be derived from the unsteady, ideal diffusion equation for lithium in a spherical particle:

$$\frac{\partial C_{\mathrm{Li}}}{\partial t} = \frac{1}{r^2}\frac{\partial}{\partial r}\left(r^2 D_{\mathrm{Li}}\frac{\partial C_{\mathrm{Li}}}{\partial r}\right), \tag{1}$$

where C_{Li} is the local lithium concentration, t is the time, r is the distance from the center of the particle, and D_{Li} is the lithium diffusion coefficient. For a GITT rest step, this equation is subject to the boundary conditions:

$$\left.\frac{\partial C_{\mathrm{Li}}}{\partial r}\right|_{r=0} = 0, \tag{2}$$

$$\left.\frac{\partial C_{\mathrm{Li}}}{\partial r}\right|_{r=R_p} = 0, \tag{3}$$

where R_p is the radius of the particle. This system can be rewritten and solved as an eigenvalue problem:

$$C_{\mathrm{Li}}(r,t) = \frac{\rho(r)\,\tau(t)}{r}, \tag{4}$$

$$\frac{1}{\tau}\frac{d\tau}{dt} = -\lambda, \tag{5}$$

$$D_{\mathrm{Li}}\frac{d^2\rho}{dr^2} + \lambda\rho = 0, \tag{6}$$

$$\rho(r=0) = 0, \tag{7}$$

$$\left.\frac{d}{dr}\left(\frac{\rho}{r}\right)\right|_{r=R_p} = 0, \tag{8}$$

where λ is the eigenvalue for the system. Solving the equation system for ρ as an ordinary differential equation gives a non-trivial solution subject to the eigenvalue constraint:

$$\tan\left(R_p\sqrt{\frac{\lambda}{D_{\mathrm{Li}}}}\right) = R_p\sqrt{\frac{\lambda}{D_{\mathrm{Li}}}}, \tag{9}$$

which can be solved numerically for the first, non-trivial root as:

$$\lambda = \frac{20.2 D_{\mathrm{Li}}}{R_p^2}. \tag{10}$$

Substituting this root into Eq. (5) and knowing that the lithium concentration will approach a homogeneous concentration $C_{\mathrm{Li},\infty}$ at long times, one can solve for τ to obtain a solution for the transient behavior of the lithium concentration:

$$C_{\mathrm{Li}} - C_{\mathrm{Li},\infty} = k_1 \exp\left(-\frac{20.2 D_{\mathrm{Li}}}{R_p^2} t\right), \tag{11}$$

where k_1 is a proportionality constant with respect to time.

During the rest step, the surface voltage of the particle will be a function f of the surface lithium concentration. Differentiating the logarithm of the difference of this function from its homogeneous state with respect to time gives:

$$\frac{d}{dt}\left\{\ln\left[f\left(C_{\mathrm{Li}}\right) - f\left(C_{\mathrm{Li},\infty}\right)\right]\right\} = \frac{\frac{d}{dt}\left[f\left(C_{\mathrm{Li}}\right)\right]}{\left[f\left(C_{\mathrm{Li}}\right) - f\left(C_{\mathrm{Li},\infty}\right)\right]}, \tag{12}$$

where the derivative of the $f\left(C_{\mathrm{Li},\infty}\right)$ term in the numerator may be canceled because $C_{\mathrm{Li},\infty}$ is a constant. Eq. (12) may be simplified further by using Eq. (11) and the chain rule for differentiation:

$$\frac{d}{dt}\left\{\ln\left[f\left(C_{\mathrm{Li}}\right) - f\left(C_{\mathrm{Li},\infty}\right)\right]\right\} = -\lambda \frac{d}{dC_{\mathrm{Li}}}\left[f\left(C_{\mathrm{Li}}\right)\right] \frac{k_1 \exp\left(-\lambda t\right)}{\left[f\left(C_{\mathrm{Li}}\right) - f\left(C_{\mathrm{Li},\infty}\right)\right]}. \tag{13}$$

If we assume the lithium concentration is close to homogeneous in the particles (i.e. at long times), the reciprocal of the rightmost term in Eq. (13) can be approximated as the derivative of f with respect to C_{Li}, using the definition of the derivative:

$$\frac{d}{dC_{\mathrm{Li}}}\left[f\left(C_{\mathrm{Li}}\right)\right] \approx \frac{\left[f\left(C_{\mathrm{Li}}\right) - f\left(C_{\mathrm{Li},\infty}\right)\right]}{\left[k_1 \exp\left(-\lambda t\right) + C_{\mathrm{Li},\infty}\right] - C_{\mathrm{Li},\infty}}. \tag{14}$$

Applying this simplification and substituting in the overpotential $\eta = f(C_{\mathrm{Li}}) - f(C_{\mathrm{Li},\infty})$, we obtain:

$$\frac{\partial \ln(\eta)}{\partial t} = -\lambda = -\frac{20.2 D_{\mathrm{Li}}}{R_p^2}. \tag{15}$$

Additional Experimental Details

We performed a cross-section SEM image of the FeS_2 slurry electrode, shown in Fig. S1, to determine the thickness. Based on our results, we estimate the thickness to be approximately 30 µm. Historically, FeS_2 exhibits significantly different voltage profiles depending on the cycling protocol. To alleviate this issue and isolate the intercalation region for FeS_2, we restricted the voltage window to be between 1.6-2.4 V. In addition to allowing us to isolate the intercalation regime, by restricting the voltage window, we avoid the significant capacity fade that occurs and is associated with the upper conversion plateau for the full 1-3 V window.[1,2] A demonstration of the improved cycling performance and comparison to the first lithiation and partial delithiation is shown in Fig. S2. We also include the experimental checklist from Sun[3] for our study shown in Fig. S3.

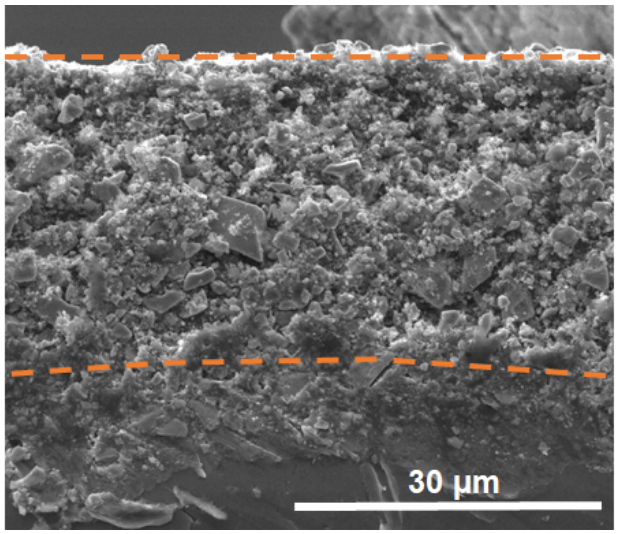

Figure S1: **Cross-section SEM image of the FeS_2 slurry electrode.** Thickness of the slurry is approximately 30 µm

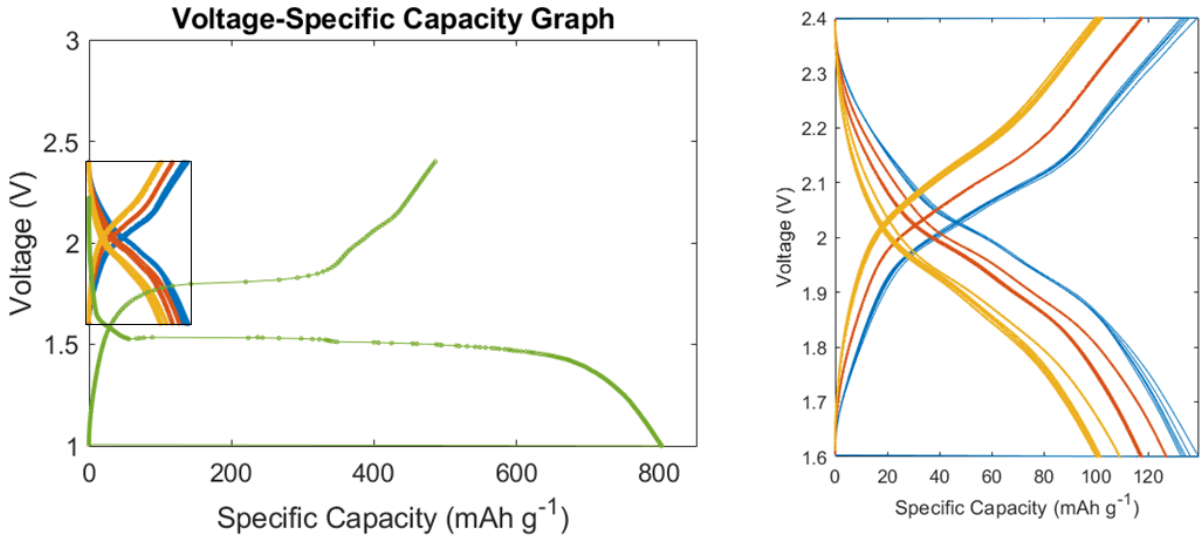

Figure S2: **Isolation of the intercalation region.** To isolate the intercalation region, FeS_2 was first lithiated down to 1 V and partially delithiated up to 2.4 V at (green) C/50. From this point, the voltage window was limited to 1.6-2.4 V and cycling was performed at (blue) C/20, (orange) C/10, and (yellow) C/5.

60 °C GITT Measurements and Analysis

In addition, we also performed the same experiments on FeS_2 at 60 °C, subject to the same protocol described in the main text. The experimental results for the intercalation region are presented in Fig. S4a. For the 60 °C experiments, the voltage was limited to 2.3 V rather than 2.4 V, due to the lower overpotential for the upper conversion reaction at 60 °C. We hypothesize that this lower overpotential is due to lower charge transfer resistance at elevated temperatures. Differences in the capacity between the room temperature and 60 °C cells are believed to originate from variations in the fabrication process. The same analysis methods used in the main text to obtain the room temperature intercalation data were performed to evaluate the lithium diffusion coefficients in FeS_2 at 60 °C. The resulting diffusion coefficients (as estimated from the non-ideal and ideal direct-pulse fitting methods) are shown in Fig. S4b and compared to the results for the room temperature measurements. As expected, the diffusion coefficients at 60 °C are higher than those obtained from room temperature data. However, the magnitude of this difference decreases with increasing capacity,

	Confirmed	N/A	Additional comments
Battery assembly	☑	☑	
Design of cell structure (e.g., 2032-coin cell, 3 cm * 5 cm pouch type cell, or others)	√		2032 coin cell
The relative weights of the active materials, conducting agent, and binder in an electrode	√		80 AM:10 Super P:10 PVDF
The loading level of the active material (mg/cm^2) in the electrode	√		~1-1.5 mg/cm^2
The capacity balance between the cathode and anode (N/P) in a full cell		N/A	
Lithium metal thickness and size (lithium metal cells)		N/A	
Composition of electrolyte and details of additives	√		1M LiFSI $PYR_{14}TFSI$
The amount the electrolyte and the ratio of electrolyte to active material.	√		80 µL
Specifications of used materials (amount in grams, purity, concentration, vendor, etc.)	√		Mass and vendor provided
Evaluation of electrochemical performance	☑	☑	
Type of cell (half or full cells) used for the electrochemical tests	√		
Number of the stacked electrodes and the corresponding total capacity (full cells)		N/A	
Cell capacity (mAh) or areal capacity (mAh/cm^2)	√		Mass + theoretical capacity provided
Theoretical capacity to determine C-rate and C-rate for each electrochemical test	√		
The range of the operating voltage	√		
The ambient temperature during electrochemical evaluations			
Specified C-rate for each electrochemical test	√		
First cycle or initial pre-cycling conditions and electrochemical data	√		
Initial charge–discharge Ah efficiency and the capacity evaluated at a low C-rate (e.g., 0.1 C)		N/A	we are only partially delithiating to 2.4 V
Pressure applied to the cell (if additional pressure is applied during cycling)		N/A	
Method of calculation of energy density (material, electrode, cell, pack level, etc.)		N/A	
Electrochemical testing procedures and CC/CV mode	√		

Figure S3: **Experimental checklist for results presented in this work.**

which could suggest a change in the reaction mechanism at higher capacities. By evaluating diffusion coefficients at both room temperature and 60 °C, we provide a starting point for non-isothermal studies, although more comprehensive data are required to construct a scaling relation for the diffusion coefficients with respect to temperature.

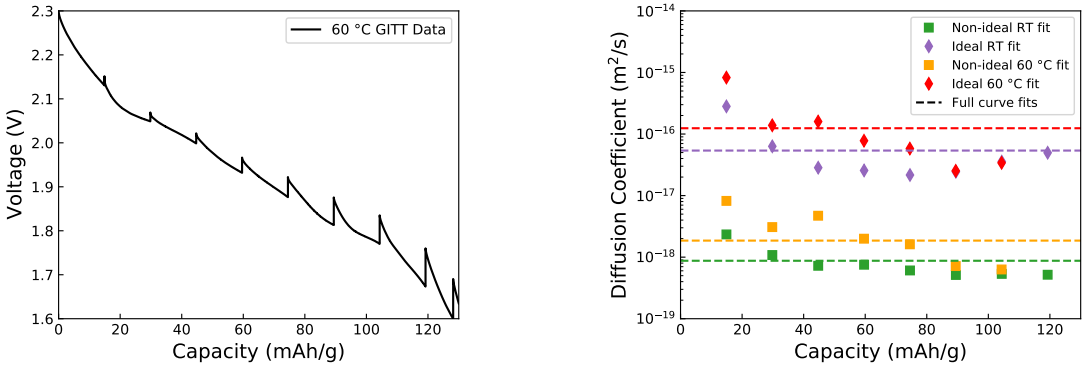

Figure S4: **FeS_2 measurements and evaluated diffusion coefficients at** 60 °C. (a) Experimental GITT data for the intercalation regime of FeS_2 at 60 °C. (b) Comparison of room temperature and 60 °C optimal diffusion coefficients evaluated through the direct-pulse fitting method. Points represent individual pulse fits, and lines represent full curve fits.

EIS Measurements and Analysis

As a comparison to the GITT-derived diffusion coefficients, electrochemical impedance spectroscopy (EIS) was performed on similarly prepared cell at room temperature and 60 °C. To obtain the diffusion coefficients, EIS was performed every hour on a 1 mg/cm^2 loading cell cycled at C/20 (1C=725 mA/g) for two cycles. Before each EIS collection, the system was allowed to rest for 5 minutes (Fig. S5a). An examplar EIS plot is provided, with the corresponding Randles circuit to fit the data (Fig. S5b). The diffusion coefficients were extracted from the Warburg coefficient obtained from the fitted EIS data (Fig. S5c) during delithiation using a previously established model.[4] The calculated diffusion coefficients correlate well to the ideal values calculated from GITT for both temperatures (Fig. S4b), similar to results in previous studies that compared diffusion coefficient extraction techniques in lithium-ion

electrodes.[5,6] This deviation of the EIS values from the non-ideal is unsurprising, due to the uncertainty of variables (i.e. the active surface area not being in equilibrium and the ambiguity of the Warburg coefficient), which can be misinterpreted by overlap with the elements representing diffusion through the porous cathode. As such, while the diffusion coefficients calculated from the EIS circuit correspond well to the traditionally calculated GITT coefficient, the assumptions used in the EIS model can lead to a high degree of uncertainty,[7] especially when moving to more complex systems. The uncertainty surrounding EIS-derived diffusion coefficients highlights the importance of moving beyond the currently used generalized-diffusion-extraction techniques, particularly as electrochemical redox mechanisms become more complex.

NCM523 GITT Interpretation

We obtained NCM523 experimental particle size distribution and charging GITT data from Nickol et al.[8], and we employed the same methodology described in the main text for FeS_2. The relevant parameters used for NCM523 are listed in Table S1. Values for the NCM523 theoretical capacity and maximum lithium concentration were taken from Verma et al.[9]. The OCV was evaluated from exponential extrapolation of the rest steps, as explained in the main text. We fit the particle distribution to a Weibull distribution with shape and scale parameters of 2.51 and 7.59 µm, respectively, and we simulated 50 particles for the polydisperse simulations. Additionally, we applied the direct-pulse fitting method to a single-particle with a radius of 5 µm, which was the assumed radius used for the GITT analysis in the original paper. For reference, the diffusion coefficients obtained by Nickol and coworkers ranged from approximately $4 \times 10^{-16}\,\mathrm{m^2/s}$ to $1 \times 10^{-15}\,\mathrm{m^2/s}$.

Our analysis for NCM523 demonstrates that estimated diffusion coefficients from experimental GITT data can vary over orders of magnitude. In particular, discrepancies may arise from inaccurate estimation of the effective particle radius, where we observed an approxi-

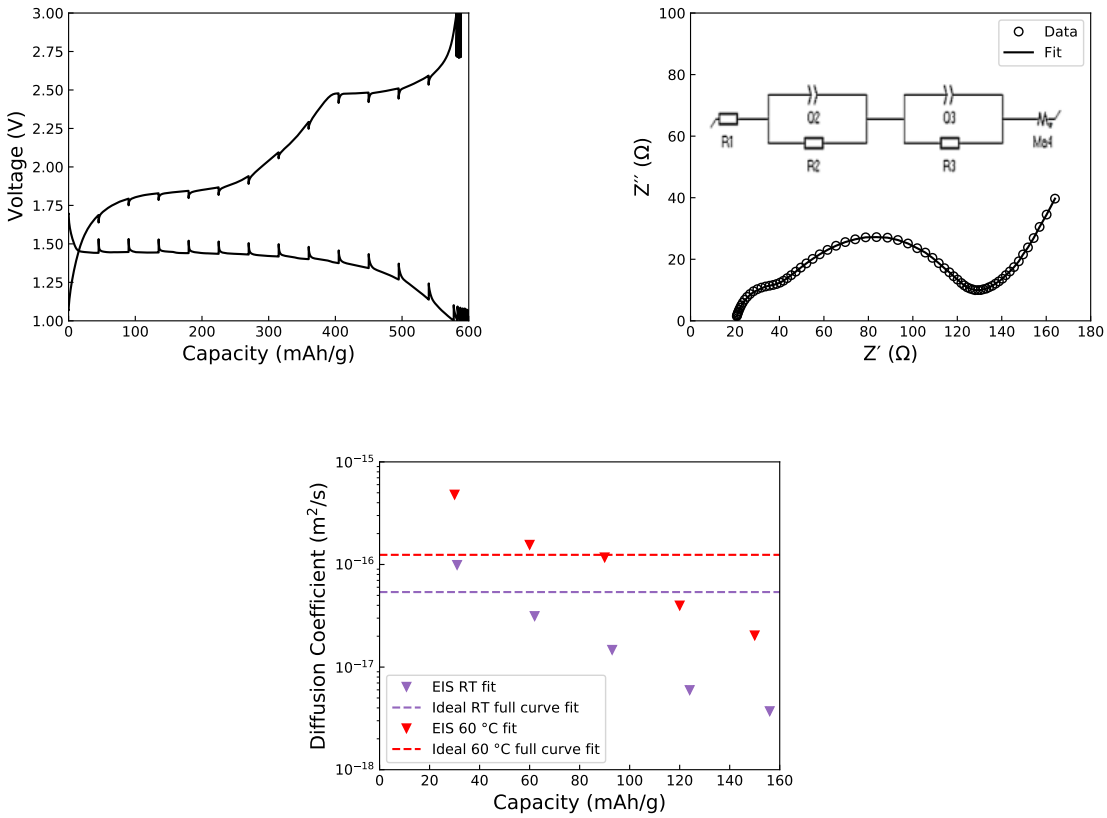

Figure S5: **EIS analysis of FeS_2.** (a) Demonstrative 1st charge and discharge at room temperature for FeS_2 cycled at C/20. EIS was obtained every hour after a 5 minute rest for the 1st and subsequent cycles. (b) (symbols) Example EIS data (line) fitted with the inset circuit. Ma represents a modified Warburg element to account for the constant phase element. The RC circuits represent the charge transfer mechanism for the anode and cathode. (c) Diffusion coefficients extracted for the FeS_2 intercalation region at room temperature (RT) and 60 °C. The dotted lines correspond to the ideal GITT coefficient, full curve fits.

Table S1: Relevant NCM523 parameters used in the model fitting and predictions.

Parameter	Description	Value
F	Faraday constant	96 485 C/mol
α	Charge transfer coefficient	0.5
R	Ideal gas constant	8.314 J/(K mol)
T	Temperature	303 K
$C_{\mathrm{Li+}}$	Electrolyte concentration	1000 mol/m^3
$C_{\mathrm{max,Li}}$	Maximum lithium concentration	48 230 mol/m^3
c_{max}	Theoretical capacity	275.62 mA h/g
x_0	Initial x in $Li_xNi_{0.5}Co_{0.2}Mn_{0.3}O_2$	0.9
R_p	Particle radius (unless otherwise specified)	5 µm

mately four-fold increase in estimated diffusion coefficients obtained using the full distribution compared to diffusion coefficients obtained using an assumed particle radius of 5 µm. Furthermore, discrepancies may also arise depending on the method used to evaluate the diffusion coefficients. Using the direct-pulse fitting method, we obtained higher diffusion coefficients than any estimated in the original paper, even when the same effective particle radius was used. Lastly, discrepancies can also arise depending on the assumed diffusion model. Consistent with our results in the main text, we obtained ideal diffusion coefficients that were more than an order of magnitude larger than those obtained for non-ideal solution theory, which generalizes our conclusion that a fundamental difference exists between ideal and non-ideal diffusion coefficients for intercalation cathode materials.

References

(1) Zou, J.; Zhao, J.; Wang, B.; Chen, S.; Chen, P.; Ran, Q.; Li, L.; Wang, X.; Yao, J.; Li, H.; Huang, J.; Niu, X.; Wang, L. Unraveling the Reaction Mechanism of FeS2 as a Li-Ion Battery Cathode. *ACS Applied Materials & Interfaces* **2020**, *12*, 44850–44857.

(2) Evans, T.; Piper, D. M.; Kim, S. C.; Han, S. S.; Bhat, V.; Oh, K. H.; Lee, S.-H. Ionic Liquid Enabled FeS2for High-Energy-Density Lithium-Ion Batteries. *Advanced Materials* **2014**, *26*, 7386–7392.

(3) Sun, Y.-K. An Experimental Checklist for Reporting Battery Performances. *ACS Energy Letters* **2021**, *6*, 2187–2189.

(4) Liao, X.-Z.; Ma, Z.-F.; Gong, Q.; He, Y.-S.; Pei, L.; Zeng, L.-J. Low-temperature performance of LiFePO4/C cathode in a quaternary carbonate-based electrolyte. *Electrochemistry Communications* **2008**, *10*, 691–694.

(5) Yu, P.; Popov, B. N.; Ritter, J. A.; White, R. E. Determination of the Lithium Ion

Diffusion Coefficient in Graphite. *Journal of The Electrochemical Society* **1999**, *146*, 8–14.

(6) Rho, Y. H.; Kanamura, K. Li+ ion diffusion in Li4Ti5O12 thin film electrode prepared by PVP sol–gel method. *Journal of Solid State Chemistry* **2004**, *177*, 2094–2100.

(7) THOMAS, M.; BRUCE, P.; GOODENOUGH, J. Lithium mobility in the layered oxide Li1-xCoO2. *Solid State Ionics* **1985**, *17*, 13–19.

(8) Nickol, A.; Schied, T.; Heubner, C.; Schneider, M.; Michaelis, A.; Bobeth, M.; Cuniberti, G. GITT Analysis of Lithium Insertion Cathodes for Determining the Lithium Diffusion Coefficient at Low Temperature: Challenges and Pitfalls. *Journal of The Electrochemical Society* **2020**, *167*, 090546.

(9) Verma, A.; Smith, K.; Santhanagopalan, S.; Abraham, D.; Yao, K. P.; Mukherjee, P. P. Galvanostatic Intermittent Titration and Performance Based Analysis of LiNi0.5Co0.2Mn0.3O2Cathode. *Journal of The Electrochemical Society* **2017**, *164*, A3380–A3392.